archives
of thermodynamics
Vol. **44**(2023), No. 3, 161–177
DOI: 10.24425/ather.2023.147542

Emissivity measurement of black paint using the calorimetric method

EWA PELIŃSKA-OLKO*

Wrocław University of Science and Technology, Faculty of Mechanical and Power Engineering, Department of Thermodynamics and Renewable Energy Sources, Wybrzeże Wyspiańskiego 27, 50-370 Wrocław, Poland

Abstract The paper is of practical importance and describes the construction of a test rig and the measurement method for determining the relative emissivity coefficient of thermosensitive thin polymer coatings. Polymers are high-molecular chemical compounds that produce chains of repeating elements called 'mers'. The polymers can be natural and artificial. The former ones form the building material for living organisms, the latter – for plastics. In this work, the words plastics and polymers are used as synonyms. Some plastics are thermosensitive materials with specific physical and chemical properties. The calorimetric method mentioned in the title consists of two steps. The first stage, described here, involves very accurately measuring the emissivity of black paint with the highest possible relative emissivity coefficient, which covers the surface of the heater and the inner surface of the chamber. In the second step, the thermosensitive polymer will be placed on the inner surface of the chamber, while black paint with a known emissivity coefficient will remain on the heater. Such a way of determining the properties of thermosensitive polymers will increase the error of the method itself, but at the same time will avoid melting of the polymer coating. During the tests, the results of which are presented in this work, the emissivity coefficient of the black paint was obtained in the range of 0.958–0.965.

Keywords: Calorimetric method; Emissivity; Thermosensitive materials; Polymers; Plastics

*Corresponding Author. Email: ewa.olko@pwr.edu.pl

Nomenclature

c_p – specific heat at constant pressure, J/(kgK)
S – surface, m^2
P – power, W
T – temperature, K

Greek symbols

ρ – mass density, kg/m^3
ε – emissivity coefficient
$\dot{Q}$ – heat stream, W

1 Introduction

This paper presents the design of the test rig and the results of the first stage of the study of the relative emissivity coefficient, understood as the amount of thermal radiation as a form of energy transferred between solids of different temperatures – in the energy and electromagnetic wavelength range: from 1 μeV to 1 eV and 10^{-6} m to 10^{-3} m, respectively. The solids studied in the second stage will belong to a special group of materials that have a low softening point or clearly change their thermophysical properties with temperature. The measurement of certain properties, including emissivity in the method presented here, ultimately requires that samples of thermosensitive materials be placed at low temperatures, below the softening point.

This group of materials includes plastics, which are used as insulation, whether in the form of rigid surfaces , films or directly sprayed onto a specific body [1–3]. The coatings change surface heat transfer coefficients similarly to ceramic coatings in blast furnaces and exchangers operating at high temperatures [4]. Plastics appear to be the materials of the future [5]. They are both transparent and opaque. Without chemical admixtures, they generally have low thermal conductivity [6]. They are very popular in the construction industry [7,8], and because they can also be transparent, they are used to achieve high thermal yields, in buildings with walls with so-called high optical efficiency [9]. Mention should also be made of the so-called solar energy market, where plastics are increasingly competing with glass or metal structural elements in various solar devices due to their relatively low weight and high durability. Transparent insulation increases the efficiency of devices such as solar collectors [10], built-in storage solar water heaters and others [11].

Plastic films are a group of very fast-growing materials because of the possibility of easily interfering with their properties. First of all, films can be assembled into layers with different physical and chemical properties [12], and various metals or ceramics can be sprayed onto their surface with a thickness of e.g. nanometres, thereby increasing or decreasing optical reflection or achieving selective reflection, influencing the conductivity in the layers [13] and creating other yet unexplored properties of the target materials [14], including properties affecting human health [15]. Thus, they have a variety of tasks: from reinforcing, protective - anti-burglary, increasing the insulation of building walls, and blocking UV radiation, to informative [16] and others [17]. A very good example of a common application is films used for car windows.

Such materials in general are such a rapidly growing industry that there is a need to evaluate and classify them [18].

In the practical applications of the above-mentioned ones, not only optical properties are important, but also mechanical and thermal properties, including emissivity, which justifies the topic of this paper.

In particular, some emissivity data are available in the literature, but due to the rapid development of materials, there is far too little data on these new materials. Automotive companies sometimes provide approximate emissivity values for films used for automotive glazing. However, the vast majority of such information is not published, as it is an element of commercial confidentiality. All the more so because, as mentioned earlier, plastic-polymers with relatively easily modifiable properties are increasingly used in a variety of industries, and sometimes form their basis. Therefore, topics related to the study of the properties of thin surfaces made of different types of polymers are very topical now and in the future. However, as mentioned earlier, these types of materials require a special approach when studying their properties.

Emissivity measurement methods can be briefly divided into two main groups: radiometric and calorimetric methods. The first group includes methods that use the information provided by infrared radiation in a selected range of electromagnetic waves by an infrared detector installed most often in a thermal imaging camera. This camera measures and then images the radiation coming from the object being photographed. The energy that can be measured in this way is a function not only of the object's temperature but also of its emissivity. Therefore, when using methods with thermal cameras, radiometric calibration of such devices is essential. The accuracy of the results obtained depends on the correct application of the appro-

priate measurement procedures [19–23] the authors present the design and operating principles of polarimetric imaging cameras.

The calorimetric method of measuring emissivity is classified as a conventional method. It involves direct heating of the sample and the emissivity is determined from the measured temperature and surface area of the sample, as well as the electrical power converted into radiation and consumed in the heating process under specified conditions – often in a vacuum. The system under test is brought to thermodynamic equilibrium with the measurement of specific parameters under so-called steady-state conditions. Samples should therefore be characterised by good thermal conductivity [24].

There are also variants of calorimetric methods that use measurements over a specific time interval, in transient states, the so-called dynamic methods, which require further mathematical calculations to determine the values of specific parameters in the distant future, e.g. using neural networks. Again, material samples should generally have good thermal conductivity, but practically, the method has also been shown to be effective for materials with lower thermal conductivity. In [25] a variation of the calorimetric method was used to measure the properties of non-metallic materials, which are not electrically self-heating. A Fourier transform spectrometer (FTS) was used on the test bench. One calorimetric method has also been successfully used to measure the properties of thin polyamide films, which are poor heat conductors too [26].

It is also possible to combine methods from both of these main groups [27].

In short: the advantage of the calorimetric method is that the value of the selected parameter can be determined in a steady state, the value of which is assumed to be constant in time. In addition, test stands built using this method usually have a relatively simple and logical construction. The disadvantage of this method is the high operating costs resulting from the need to create certain constant conditions both inside and outside the measuring station for a relatively long time.

The use of the calorimetric method in this work was determined by the above-mentioned advantages and the fact that most of the values of material parameters applicable in technology are determined in steady states.

The calorimetric method proposed here consists of establishing a heat balance while continuously heating a rectangular radiator inside a hexagonal chamber placed inside a desiccator, hereafter referred to as the chamber. During the test, the air is pumped out of the desiccator using a vacuum pump to eliminate heat transfer by convection. The only form of energy exchanged between the heater and the internal surface of the chamber is therefore radiant energy.

2 Theory

Heat radiation has the same properties as light waves in the spectrum visible to the eye. The condition for heat exchange in this way is the presence of a transparent medium between bodies of different temperatures exchanging energy with each other. The useful formulas used in this work are based on laws discovered in the course of radiation research. These are primarily Planck's law, formulated as a formula for the amount of radiation emitted by a blackbody as a function of the electromagnetic wavelength emitted and the temperature of the body, and Stefan-Boltzman's law, which describes the total energy flux radiated by a blackbody. In its simplest form, the amount of energy radiated from a body with temperature T expressed in kelvins into a vacuum, is proportional to the fourth power of the absolute temperature of that body. A black body is characterised by the fact that, at steady-state, it absorbs as much energy as it radiates. Grey bodies, found in the real world, radiate similarly to black bodies over the entire wavelength range, only slightly weaker. To compare the radiation properties of a gray body with a black body, the concept of relative emissivity coefficient is introduced, i.e. the quotient of the amount of energy radiated by a gray body to the amount of energy radiated by a perfect black body at a given temperature. The value of this coefficient may refer to a specific length of the emitted electromagnetic wave or to its average value determined by the appropriate temperature range. According to the literature, the emissivity of all bodies is not greater than the one.

The idea of the calorimetric measurement method shown in Fig. 1 is based on radiative heat transfer from the rectangular heater (2) to the

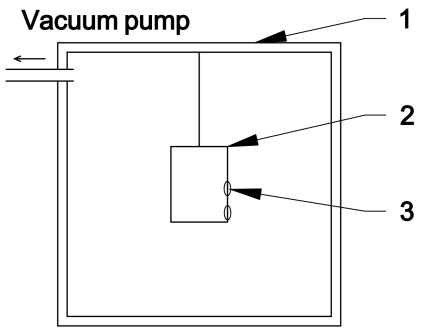

Figure 1: Conceptual outline of a test rig for testing the emission of back paint and coatings of thermosensitive materials.

cooler surface of the cubic chamber (1) surrounding it, hereinafter referred to as the chamber. The temperature will be read by means of thermocouples (3) located on the surface of the heater and the chamber. Both the chamber and the heater are placed inside the vacuum desiccator to eliminate heat transfer by convection.

Measurements will be carried out in two stages. The first stage, described here, involves measuring the emissivity of the black paint that covers both the surface of the heater and the inner surface of the chamber. The coating used, which is also an example of a polymer, has sufficient thermal resistance to be placed on the heater.

Using equations (1), (2) known from the literature [28–31], it is possible to calculate the relative emissivity coefficient under the conditions of thermal equilibrium of the system:

$$\varepsilon_z = \frac{\dot{Q}_{1-2}}{S_1 \sigma \left[(T_1)^4 - (T_2)^4 \right]}, \tag{1}$$

$$\varepsilon_z = \frac{1}{\dfrac{1}{\varepsilon_1} + \dfrac{S_1}{S_2}\left(\dfrac{1}{\varepsilon_2} - 1\right)}, \tag{2}$$

where: ε_z – the so-called equivalent relative emissivity coefficient obtained experimentally without taking into account the position of the surfaces exchanging heat with each other, $\dot{Q}_{1-2}$ – heat stream exchanged between surfaces with different temperature, S_2, S_2 – the outer surface of the heater and the inner surface of the chamber respectively, T_1, T_2 – the higher and the lower average absolute temperature respectively, σ – Stefan–Boltzmann constant, ε_1, ε_2 – emissivity coefficients for surfaces with temperatures T_1 and T_2 respectively.

In the presence of black paint on the surface of the chamber and the heater, from (2) the following formula can be obtained (3):

$$\varepsilon_1 = \frac{1 + \dfrac{S_1}{S_2}}{\dfrac{1}{\varepsilon_z} + \dfrac{S_1}{S_2}}, \tag{3}$$

where: ε_1 – the relative emissivity coefficient of black paint, assuming its equal emissivity on the surface of the heater and the inner surface of the chamber.

The emissivity coefficient of the black paint determined in this way has a smaller absolute error than if the heater and the interior of the chamber were covered with different coatings. It is calculated using the differential method, which is presented later in this paper. Its smaller value is due to the smaller number of components affecting the value of the total error associated with this method. Knowledge of the relative emissivity of the black paint described above is necessary to determine the emissivity of the corresponding temperature-sensitive material in the second stage of the study.

3 The construction of the test rig

The test rig, shown schematically in Fig. 1, was originally built to assess the correctness of neural networks for predicting the temperature of heated solids in the distant future, which in practice meant determining the steady-states temperature at specific points on the body. The photograph with main components of the rig can be found in the article [32]. It has been adapted to determine the relative emissivity of black paint, mentioned in the title of the work and allows a proper thermal equilibrium to be achieved.

The ambient test conditions are a dynamic vacuum of 300 Pa (2500 μmHg). Inside the desiccator, which acts as a vacuum chamber, is a cube made of 5 mm thick sheet metal with 150 mm sides. Its interior forms a closed space, hereinafter referred to as the chamber, with an inner side length of 140 mm, made of PA11 aluminium alloy with a linear thermal expansion coefficient of $23.7 \cdot 10^{-6}$ 1/K. In its geometrical centre was placed a rectangular heater made of PA6 aluminium alloy with a linear coefficient of thermal expansion of $22.9 \cdot 10^{-6}$ 1/K. The heater was made of a rod with a square cross-section, side $a = 30$ mm. The heater has a length of $b = 40$ mm. The design of the heater is simple. A resistance wire (Fe Cr Al 135), insulated with Teflon, is wound on a threaded aluminium alloy pivot with a diameter of approximately 25 mm. The resistance wire has a diameter of $d = 0.5$ mm and a resistance of Ω/m.

The pivot is placed in a hole in a square rod, which forms the body of the heater. Its average resistance at room temperature 20°C is 9.667 Ω. The resistance of the cables connecting the heater with the power supply at 20°C is 0.037 Ω. The test rig is attached to a gauge of type KEITHLEY (hereinafter called the gauge), which provides relatively accurate readings of output signals in the form of resistance or voltage.

4 The way of performing the measurements

On the test rig, temperatures were measured at three specified locations on the heater and three specified locations on the inner surface of the chamber (Fig. 2).

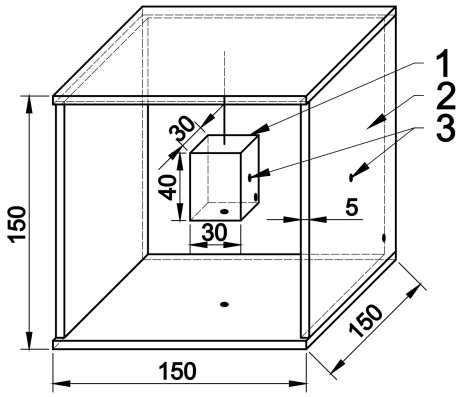

Figure 2: Axonometric mapping of the interior of the chamber (2) including the heater (1) and temperature measurement locations (3).

Temperature measuring points on the heater are located at the intersection of the diagonals: one on the side wall, one on the bottom wall, and one in the corner of the side wall. Similarly, three measurement points are defined on the inner walls of the chamber. The temperature was measured with thermocouples after they had been calibrated: [33–35]. An average temperature was then calculated on the heater and on the surface of the chamber, which was treated as a constant value, for a given power dissipated by the heater.

The reference temperature of cold ends of thermocouples in the temperature of the meter is measured by the PT-1000 resistance sensor calibrated earlier [36]. During each experiment, the voltage and resistance in the heater circuit were measured. The pressure in the desiccator was maintained at 300 Pa using a vacuum pump. This is known as a dynamic vacuum, which requires continuous operation of the vacuum pump.

Two stages of the process can be distinguished in each experiment. In the first stage, the desiccator was filled with air at ambient pressure. The temperature stabilization process after switching on the heater was relatively quick. After about 30% of the duration of the entire experiment, the second stage occurred, in which the vacuum pump was turned on and

operated until the steady state temperature was reached at selected measurement points.

5 The test results

A sample temperature evolution on selected surfaces at the test rig is shown in Fig. 3.

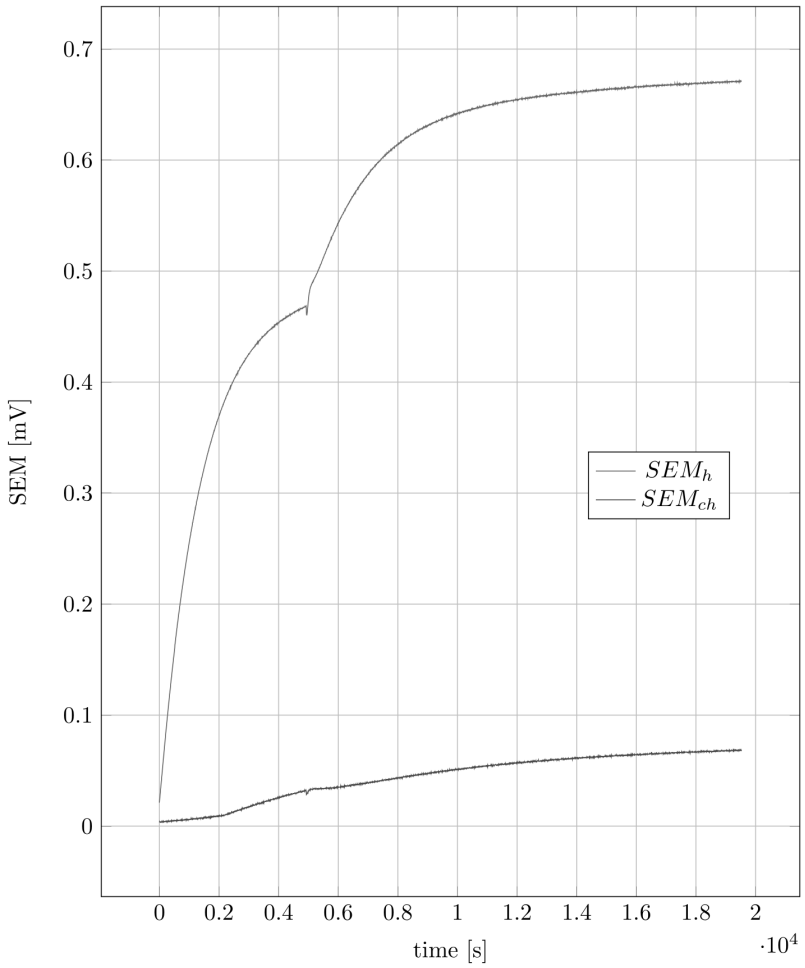

Figure 3: The dependence of the average temperature from time, exspressed in SEM_h on the heater (higher values) and in SEM_{ch} on the inner surface of the chamber (lower values).

The heat flux dissipated by the heater $\dot{Q}_{1-2}$ (4) is power on the heater P minus two kinds of losses. One is the loss on the wires $\dot{Q}_w$, which can be estimated using the Fourier formula, based on knowledge of the diameters of the thermocouples wires and the temperature difference between the surfaces on which the measuring junctions are placed and the environment in which the meter is located. Another one is the loss of enthalpy $\dot{Q}_v$ in the chamber resulting from the maintenance of dynamic vacuum at 300 Pa. Therefore:

$$\dot{Q}_{1-2} = P - \dot{Q}_w - \dot{Q}_v \,. \tag{4}$$

Examples of experimental results are given in Table 1. Here the following information is gathered in columns from left to right: the ambient temperature where the gauge is placed, measured by Pt-1000 thermometer; the heat stream dissipated by the heater, taking into account losses (4); the resistance of the hot heater; voltage in the heater circuit; SEM of thermocouples measured in the corresponding points of the heater and the inner surface of the chamber: ΔT_1–ΔT_6; the average temperature of the heater T_{avh} and the inner surface of the chamber T_{avch}; the relative emissivity coefficient ε_z, ε_1, $\varepsilon_2 = \varepsilon_1$; the absolute method error $\Delta\varepsilon$.

Table 1: The selected experimental results gathered during the emissivity measurement.

File		1	2	3	4	5	6
t_0	K	296.313	290.405	292.503	292.668	289.695	291.506
$\dot{Q}_{1-2}$	W	0.219	0.758	1.338	1.336	2.17	5.057
R	Ω	9.686	9.797	9.685	9.709	9.788	9.808
U	V	1.462	2.748	3.604	3.613	4.626	7.065
ΔT_1	mV	4.159	16.387	26.593	26.235	41.733	77.775
ΔT_2	mV	4.035	16.134	24.87	25.835	40.389	80.63
ΔT_3	mV	4.374	15.895	25.855	25.899	39.719	76.468
ΔT_4	mV	0.552	1.979	2.812	3.363	4.915	12.071
ΔT_5	mV	0.29	1.727	2.996	2.847	4.676	8.767
ΔT_6	mV	0.156	1.17	1.875	1.723	3.611	9.344
$T_{av\,h}$	K	300.543	306.583	318.632	318.699	330.349	369.837
$T_{av\,ch}$	K	296.687	292.07	295.421	295.353	294.136	301.607
ε_z		1.052	0.954	0.975	0.973	0.961	0.955
ε_1		1.049	0.958	0.976	0.975	0.964	0.958
$\Delta\varepsilon$		0.102	0.027	0.017	0.017	0.012	0.07

6 Errors in determining the emissivity of black paint

The method adopted in the experiment for determining the relative emissivity coefficient is the classical calorimetric method. In the direct measurement, the temperature at the selected locations, the current and voltage supplying the heater, the vacuum level in the desiccator, the corresponding areas of the heater and the interior surface of the chamber, and the ambient temperature and pressure are measured. When both the heater and the inner surface of the chamber are covered with black paint, the formula for the relative emissivity coefficient of this material is of the form (5):

$$\varepsilon_1 = \frac{\dfrac{U^2}{R}\left(1+\dfrac{S_1}{S_2}\right)}{CS_1\left[\left(\dfrac{T_1}{100}\right)^4-\left(\dfrac{T_2}{100}\right)^4\right]+\dfrac{S_1U^2}{S_2R}}, \tag{5}$$

where: ε_1 – the relative emissivity coefficient of the black paint, U, R – the voltage and the resistance of the heater, respectively, S_1, S_2 – the surface of the heater and the inner surface of the vacuum chamber, respectively, T_1, T_2 – the measured average temperature of the heater and the inner surface of the chamber, respectively, $C = 5.67\ \mathrm{W/(m^2K^4)}$.

The maximum error of the method was determined by summing the absolute values of the errors of the individual quantities occurring in the (5). The individual members generating absolute errors have the form as follows:

$$\frac{\partial\varepsilon_1}{\partial U} = \frac{\dfrac{2U}{R}\left(1+\dfrac{S_1}{S_2}\right)\left\{CS_1\left[\left(\dfrac{T_1}{100}\right)^4-\left(\dfrac{T_2}{100}\right)^4\right]+\dfrac{S_1U^2}{S_2R}\right\}}{\left\{CS_1\left[\left(\dfrac{T_1}{100}\right)^4-\left(\dfrac{T_2}{100}\right)^4\right]+\dfrac{S_1U^2}{S_2R}\right\}^2} - \frac{\dfrac{U^2}{R}\left(1+\dfrac{S_1}{S_2}\right)\dfrac{S_12U}{S_2R}}{\left\{CS_1\left[\left(\dfrac{T_1}{100}\right)^4-\left(\dfrac{T_2}{100}\right)^4\right]+\dfrac{S_1U^2}{S_2R}\right\}^2}, \tag{6}$$

$$\frac{\partial \varepsilon_1}{\partial R} = \frac{-\frac{U^2}{R^2}\left(1+\frac{S_1}{S_2}\right)\left\{CS_1\left[\left(\frac{T_1}{100}\right)^4-\left(\frac{T_2}{100}\right)^4\right]+\frac{S_1U^2}{S_2R}\right\}}{\left\{CS_1\left[\left(\frac{T_1}{100}\right)^4-\left(\frac{T_2}{100}\right)^4\right]+\frac{S_1U^2}{S_2R}\right\}^2} + \frac{\frac{U^2}{R}\left(1+\frac{S_1}{S_2}\right)\frac{S_1U^2}{S_2R^2}}{\left\{CS_1\left[\left(\frac{T_1}{100}\right)^4-\left(\frac{T_2}{100}\right)^4\right]+\frac{S_1U^2}{S_2R}\right\}^2}, \tag{7}$$

$$\frac{\partial \varepsilon_1}{\partial S_1} = \left\langle IU\frac{\left\{CS_1\left[\left(\frac{T_1}{100}\right)^4-\left(\frac{T_2}{100}\right)^4\right]+\frac{S_1U^2}{S_2R}\right\}}{S_2} - \frac{U^2}{R}\left(1+\frac{S_1}{S_2}\right)\right\rangle \cdot \frac{\left\{C\left[\left(\frac{T_1}{100}\right)^4-\left(\frac{T_2}{100}\right)^4\right]+\frac{U^2}{S_2R}\right\}}{\left\{CS_1\left[\left(\frac{T_1}{100}\right)^4-\left(\frac{T_2}{100}\right)^4\right]+\frac{S_1U^2}{S_2R}\right\}^2}, \tag{8}$$

$$\frac{\partial \varepsilon_1}{\partial S_2} = \frac{-\frac{U^2}{R}\frac{S_1}{S_2^2}+\left(\frac{U^2}{R}\right)^2 S_1\left(1+\frac{S_1}{S_2}\right)\frac{1}{S_2^2}}{\left\{CS_1\left[\left(\frac{T_1}{100}\right)^4-\left(\frac{T_2}{100}\right)^4\right]+\frac{S_1U^2}{S_2R}\right\}^2}, \tag{9}$$

$$\frac{\partial \varepsilon_1}{\partial T_1} = \frac{-\frac{U^2}{R}CS_1\frac{4T_1^3}{100^4}\left(1+\frac{S_1}{S_2}\right)}{\left\{CS_1\left[\left(\frac{T_1}{100}\right)^4-\left(\frac{T_2}{100}\right)^4\right]+\frac{S_1U^2}{S_2R}\right\}^2} \tag{10}$$

$$\frac{\partial \varepsilon_1}{\partial T_2} = \frac{\frac{U^2}{R}CS_1\frac{4T_2^3}{100^4}\left(1+\frac{S_1}{S_2}\right)}{\left\{CS_1\left[\left(\frac{T_1}{100}\right)^4-\left(\frac{T_2}{100}\right)^4\right]+\frac{S_1U^2}{S_2R}\right\}^2}. \tag{11}$$

When the heater and the inner surface of the chamber are covered with coatings of different materials, the relative emissivity coefficient of the material covering the cold surface of the chamber can be calculated from the

following formula:

$$\varepsilon_2 = \frac{\dfrac{U^2}{R} s_1 \varepsilon_1}{-S_2 \dfrac{U^2}{R} + CS_1 S_2 \varepsilon_1 \left[\left(\dfrac{T_1}{100} \right)^4 - \left(\dfrac{T_2}{100} \right)^4 \right] + S_1 \dfrac{U^2}{R} \varepsilon_1} . \tag{12}$$

The corresponding partial derivatives, generating the absolute error have the following forms:

$$\frac{\partial \varepsilon_2}{\partial U} = \frac{\dfrac{2U}{R} S_1 \varepsilon_1 \left\{ -S_2 \dfrac{U^2}{R} + CS_1 S_2 \varepsilon_1 \left[\left(\dfrac{T_1}{100} \right)^4 - \left(\dfrac{T_2}{100} \right)^4 \right] + S_1 \dfrac{U^2}{R} \varepsilon_1 \right\}}{\left\{ -S_2 \dfrac{U^2}{R} + CS_1 S_2 \varepsilon_1 \left[\left(\dfrac{T_1}{100} \right)^4 - \left(\dfrac{T_2}{100} \right)^4 \right] + S_1 \dfrac{U^2}{R} \varepsilon_1 \right\}^2} - \frac{S \varepsilon_1 \dfrac{U^2}{R} \left(-S_2 \dfrac{2U}{R} + S_1 \dfrac{2U}{R} \varepsilon_1 \right)}{\left\{ -S_2 \dfrac{U^2}{R} + CS_1 S_2 \varepsilon_1 \left[\left(\dfrac{T_1}{100} \right)^4 - \left(\dfrac{T_2}{100} \right)^4 \right] + S_1 \dfrac{U^2}{R} \varepsilon_1 \right\}^2} , \tag{13}$$

$$\frac{\partial \varepsilon_2}{\partial R} = \frac{\left(-\dfrac{U^2}{R^2} \right) S_1 \varepsilon_1 \left\{ -S_2 \dfrac{U^2}{R} + CS_1 S_2 \varepsilon_1 \left[\left(\dfrac{T_1}{100} \right)^4 - \left(\dfrac{T_2}{100} \right)^4 \right] + S_1 \dfrac{U^2}{R} \varepsilon_1 \right\}}{\left\{ -S_2 \dfrac{U^2}{R} + CS_1 S_2 \varepsilon_1 \left[\left(\dfrac{T_1}{100} \right)^4 - \left(\dfrac{T_2}{100} \right)^4 \right] + S_1 \dfrac{U^2}{R} \varepsilon_1 \right\}^2} - \frac{S_1 \varepsilon_1 \dfrac{U^2}{R} \left(S_2 \dfrac{U^2}{R_2} - S_1 \dfrac{U^2}{R^2} \varepsilon_1 \right)}{\left\{ -S_2 \dfrac{U^2}{R} + CS_1 S_2 \varepsilon_1 \left[\left(\dfrac{T_1}{100} \right)^4 - \left(\dfrac{T_2}{100} \right)^4 \right] + S_1 \dfrac{U^2}{R} \varepsilon_1 \right\}^2} , \tag{14}$$

$$\frac{\partial \varepsilon_2}{\partial S_1} = \frac{\dfrac{U^2}{R} \varepsilon_1 \left\{ -S_2 \dfrac{U^2}{R} + CS_1 S_2 \varepsilon_1 \left[\left(\dfrac{T_1}{100} \right)^4 - \left(\dfrac{T_2}{100} \right)^4 \right] + S_1 \dfrac{U^2}{R} \varepsilon_1 \right\}}{\left\{ -S_2 \dfrac{U^2}{R} + CS_1 S_2 \varepsilon_1 \left[\left(\dfrac{T_1}{100} \right)^4 - \left(\dfrac{T_2}{100} \right)^4 \right] + S_1 \dfrac{U^2}{R} \varepsilon_1 \right\}^2} - \frac{S_1 \varepsilon_1 \dfrac{U^2}{R} \left\{ CS_2 \varepsilon_1 \left[\left(\dfrac{T_1}{100} \right)^4 - \left(\dfrac{T_2}{100} \right)^4 \right] + \varepsilon_1 \dfrac{U^2}{R} \right\}}{\left\{ -S_2 \dfrac{U^2}{R} + CS_1 S_2 \varepsilon_1 \left[\left(\dfrac{T_1}{100} \right)^4 - \left(\dfrac{T_2}{100} \right)^4 \right] + S_1 \dfrac{U^2}{R} \varepsilon_1 \right\}^2} , \tag{15}$$

$$\frac{\partial \varepsilon_2}{\partial S_2} = \frac{-S_1 \dfrac{U^2}{R}\varepsilon_1 \left\{ -\dfrac{U^2}{R} + CS_1\varepsilon_1 \left[\left(\dfrac{T_1}{100}\right)^4 - \left(\dfrac{T_2}{100}\right)^4 \right] \right\}}{\left\{ -S_2 \dfrac{U^2}{R} + CS_1S_2\varepsilon_1 \left[\left(\dfrac{T_1}{100}\right)^4 - \left(\dfrac{T_2}{100}\right)^4 \right] + S_1 \dfrac{U^2}{R}\varepsilon_1 \right\}^2}, \tag{16}$$

$$\frac{\partial \varepsilon_2}{\partial T_1} = \frac{-S_1 \dfrac{U^2}{R}\varepsilon_1 \left(CS_1S_2\varepsilon_1 \dfrac{4T_1^3}{100^4} \right)}{\left\{ -S_2 \dfrac{U^2}{R} + CS_1S_2\varepsilon_1 \left[\left(\dfrac{T_1}{100}\right)^4 - \left(\dfrac{T_2}{100}\right)^4 \right] + S_1 \dfrac{U^2}{R}\varepsilon_1 \right\}^2}, \tag{17}$$

$$\frac{\partial \varepsilon_2}{\partial T_2} = \frac{-S_1 \dfrac{U^2}{R}\varepsilon_1 \left(CS_1S_2\varepsilon_1 \dfrac{4T_2^3}{100^4} \right)}{\left\{ -S_2 \dfrac{U^2}{R} + CS_1S_2\varepsilon_1 \left[\left(\dfrac{T_1}{100}\right)^4 - \left(\dfrac{T_2}{100}\right)^4 \right] + S_1 \dfrac{U^2}{R}\varepsilon_1 \right\}^2}. \tag{18}$$

7 Observations and conclusions

1. Within the heater power range of 0.21–5.06 W, the relative emissivity coefficient is in the range of 0.958 ± 0.07 to 1.049 ± 0.102. The method error of determining the relative emissivity for black paint covering both the chamber interior and the heater increases with decreasing heater power.

2. Each test was performed for a different temperature range, depending on the heater power. If it is assumed that the relative emissivity coefficient of black paint is constant over the temperature range tested, then its value should fall within the common range of values of this coefficient for all the tests carried out, regardless of the accuracy of the measurements.

   The range of common values of the coefficient sought for all tests is within the field of values (0.958–0.965).

3. If the tests will include thermosensitive materials, a sample of such material should be placed on a cold surface – the inner surface of the chamber. A layer of black paint with a known value of the relative emissivity coefficient will remain on the heater. According to preliminary calculations, the error of the method should increase, but the undertaking is necessary to avoid the melting of the polymer coating.

4. After initial attempts to apply a thin thermosensitive coating on the cooler surface of the chamber, insufficiently satisfactory results were obtained in the second stage of the research. If the technical problems related to the adhesion of coatings cannot be solved, the range of materials tested by this method will be limited to those that can only be sprayed onto surfaces.

Received 17 May 2023

References

[1] Qu J., Song J.R., Qin J., Song Z.N., Zhang W.D., Shi Y.X., Shang T., Zhang H.Q., He Z.V., Xue X.: *Transparent thermal insulation coatings for energy efficient glass windows and curtain walls*. Energ. Buildings **77**(2014), 1–10.

[2] Chen Y., Wang M.D., Xu M.D., Li L.: *Preparation of AZO/acrylic resin transparent insulation coating*. Adv. Mat. Res. **369-398**(2012), 229–232.

[3] Wittwer V.: *The use of transparent insulation materials and optical switching layers in window systems*. Renew. Energ. **5**(1994), 318–323.

[4] Morel S.: *The influence of a radiated heat exchanger surface on heat transfer*. Arch. Thermodyn. **36**(2015), 3, 161–174.

[5] Paneri A., Wong I.L., Burek S.: *Transparent insulation materials: An overview on past, present and future developments*. Sol. Energy **184**(2019), 59–83.

[6] Kaushika N.D., Sumathy K.: *Solar transparent insulation materials: a review*. Renew. Sust. Energ. Rev. **7**(2003), (4), 317–351.

[7] Wong I.L., Eames P.C., Perera R.S.: *A review of transparent insulation systems and the evaluation of payback period for building applications*. Sol. Energy **81**(2007), 1058–1071.

[8] Struhala K., Cekon M., Slavik R.: *Life Cycle Assessment of solar facade concepts based on transparent insulation materials*. Sustainability-Basel **10**(2018), 11, 4212.

[9] Swirska-Perkowska J., Kucharczyk K., Wyrwal J.: *Energy efficiency of a solar wall with transparent insulation in Polish climatic conditions*. Energies **13**(2020), 4, 859.

[10] Chaurasia PBL.: *Transparent insulation material in solar system for candle production*. Energ. Convers. Manage. **41**(2020), 1569–1584.

[11] Prakash J., Garg H.P., Jha R., Hrishikesan D.S.: *Solar thermal-systems with transparent insulation*. Energ. Convers. Manage. **33**(1992), 987–996.

[12] Jia H., Zhu J.J., Debeli D.K, Li Z.L., Guo J.S.: *Solar thermal energy harvesting properties of spacer fabric composite used for transparent insulation materials*. Sol. Energ. Mat. Sol. C **174**(2018), 140–145.

[13] Tang J., Di F., Xu X., Xiao Y., Che J.: *Transparent conductive graphene films*. Prog. Chem. **24**(2012), 501–511.

[14] Kholmanov I.N., Stoller M.D., Edgeworth J., Lee W.H., Li H.F., Lee J.H., Barnhart C., Potts J.R., Piner R., Inwande Ak D., Barrick J.E., Ruoff R.: *Nanostructured hybrid transparent conductive films with antibacterial properties*. ACS Nano **6**(2012), 5157–5163.

[15] Vitelaru C., Parau AC., Kiss AE., Pana I., Dinu M., Constantin LR., Vladescu A., Tonofre L.E., Adochite C.S., Costinas S., Rogozea L., Badea M., Idomir M.E.: *Silver-containing thin films on transparent polymer foils for antimicrobial applications*. Coatings **12**(2022), 170.

[16] Froyen A.A.F., Grossiord N., Heer J., Meerman T., Yang L.T., Lub J., Schenning A.P.H.J.: *Ink-deposited transparent electrochromic structural colored foils*. ACS Appl. Mater. Inter. **14**(2022), 39375–39383.

[17] Blankenburg L., Schroedner M.: *Perhydropolysilazane derived silica for flexible transparent barrier foils using a reel-to-reel wet coating technique: Single- and multilayer structures*. Surf. Coat Tech. **275**(2015), 193–206.

[18] Syrowa L., Ravas R., Grman J.: *The use of schlieren visualization method in the diagnostic of optically transparent polymeric foils*. J. Electr. Eng. **58**(2007), 257–263.

[19] Hagen N.: *Review of thermal infrared polarimetry, I: theory*. Opt. Eng. **61**(2022), 7, 070902.

[20] Hagen N.: *Review of thermal infrared polarimetry, part 2: experiment*. Opt. Eng. **61**(2022), 8, 080901.

[21] Bieszczad G., Gogler S., Swiderski J.: *Review of design and signal processing of polarimetric imaging cameras*. Opto-Electron Rev. **29**(2021), 5–12.

[22] Kruczek T.: *Conditions for the use of infrared camera diagnostics in energy auditing of the objects exposed to open air space at isothermal sky*. Arch. Thermodyn. **36**(2015), 1, 67–82.

[23] Musiał D., Wyczółkowski R.: *Thermovision determination of the furnace chamber environment temperature using the technical black-body model*. Arch. Thermodyn. **31**(2010), 4, 25–35.

[24] Fu T.R., Tan P., Duan M.H.: *Simultaneous measurements of high-temperature total hemispherical emissivity and thermal conductivity using a steady-state calorimetric technique*. Meas. Sci. Techno. **26**(2015).

[25] Zang B., Redgrove J., Clark J.: *A transient method for total emissivity determination*. Int. J. Thermophys. **25**(2004), 423–438.

[26] Fukuzawa K., Ohnishi A., Nagasaka Y.: *Total hemispherical emittance of polyimide films for space use in the temperature range from 173 to 700 K*. Int. J. Thermophys. **35**(2002), 319–331.

[27] Vikhareva NA., Cherepanov VY.: *Radiation-calorimetric method of measurements for the thermal emissivity of heat radiators*. Meas. Tech.+ **59**(2016), 734–737.

[28] Hobler T.: *Heat Movement and Exchangers*. WNT, Warszawa 1971 (in Polish).

[29] Kostowski E.: *Heat Flow*. Wydawn. Politechniki Śląskiej, Gliwice 2006 (in Polish).

[30] Kostowski E., Górniak H., Sikora J., Szymczyk J., Ziębik A.: *A collection of tasks related to heat flow*. Wydawn. Politechniki Śląskiej, Gliwice 2003 (in Polish).

[31] Pudlik W.: *Heat Exchange and Exchangers*. Wydawn. Politechniki Gdańskiej, Gdańsk 2012 (in Polish).

[32] Pelińska-Olko E., Lewkowicz M.: *Numerical prediction of steady state temperature based on transient measurements*. In: Proc. MATEC Web Conf. **240**(2018), 05024.

[33] Wedrychowicz W.: *Thermocouple Temperature Measurement*. Wydawn. Politechniki Wrocławskiej, Wrocław 2017 (in Polish).

[34] Liu B., Huang Q.H., Wang P.Y.: *Influence of surrounding gas temperature on thermocouple measurement*. Case Stud. Therm. Eng. **19**(2020), 100627.

[35] Liu H.T., Shao D., Li B.Q.: *Theory analysis of thermocouple temperature measurement*. Appl. Mech. Mater. **239-240**(2013), 749–753.

[36] Wedrychowicz W.: *Temperature Measurement with Metal and Semiconductor Resistance Thermocouples*. Wydawn. Politechniki Wrocławskiej, Wrocław 2015 (in Polish).